J Therm Anal Calorim (2009) 97:131–136
DOI 10.1007/s10973-009-0256-4

Thermal characterization of the intermediary products of the synthesis of Zn-substituted barium hexaferrite

R. da Costa Lima · Magali Silveira Pinho · T. Ogasawara

ICTAC2008 Conference

Abstract The focus of this work is the use of thermal analyses and Fourier Transform Infrared Spectroscopy (FTIR) for characterization of the gel decomposition, resulting from the formation of Y-barium hexaferrite substituted by Zn ions (Zn-Y-barium hexaferrite). Samples with $Ba_2Zn_2Fe_{12}O_{22}$ composition were synthesized by the citrate auto-combustion method. During the TG experiments the highest mass loss was attributed to citrate decomposition owing to the self-combustion reaction, confirmed by the disappearance of –OH band, and the drastic decrease of $–CO_2^-$ and $–NO_3^-$ bands. Zn substitution resulted in an X-band microwave absorber material.

Keywords Y-type hexaferrite · Citrate sol–gel combustion method · TG · DSC

Introduction

Ferrites have continued to attract attention over the last few years. As magnetic materials, ferrites are not usually replaced because they are relatively inexpensive, chemically stable and have a wide range of technological applications such as radar absorbing materials [1, 2]. The magnetic and electrical properties of the ferrite are controlled by the preparation conditions, chemical composition, calcination temperature and time and degree of ions' substitution [3].

Barium hexaferrites have been classified according to their structures, into five main classes: $BaFe_{12}O_{19}$ (M-type), $BaMe_2Fe_{16}O_{27}$ (W-type), $Ba_2Me_2Fe_{28}O_{46}$ (X-type), $Ba_2Me_2Fe_{12}O_{22}$ (Y-type) and $Ba_3Me_2Fe_{24}O_{41}$ (Z-type), where Me represents a divalent ion from the first transition series. All Y compounds ($Ba_2Me_2Fe_{12}O_{22}$) have planar anisotropy at room temperature, regardless of the metal ion used. The different Me substitutions have a marked effect on the magnetic anisotropy and the microwave line width of the ferromagnetic resonance (FMR) [2]. In compounds with planar anisotropy like Y-type hexaferrites, ferromagnetic resonance occurs at a frequency that depends on both the applied magnetic field and the anisotropy field. In order to limit the scope of this investigation, only Zn ions were used in this work.

The classical ceramic method for preparing barium hexaferrites requires high calcination temperatures, which induces aggregation of the particles. Afterward, the milling process generally yields non homogeneous mixtures on a microscopic scale and introduces lattice strains in the materials. The use of the sol–gel technique allows achieving the homogeneity of ions at atomic level in the metallic citrate precursor complex (sol–gel precursor) and lower calcination temperature of barium hexaferrite, besides the action of the nitrate ions as an oxygen source in the gel combustion [4].

The calcination temperature can strongly affect both the FMR line width and anisotropy field. The optimum conditions according to the desirable applications should be determined by experimental studies.

R. da Costa Lima · M. S. Pinho (✉)
Brazilian Navy Research Institute (IPqM), Rua Ipiru no 2, Praia da Bica, Ilha do Governador, Rio de Janeiro, RJ 21931-090, Brazil
e-mail: magalipinho@yahoo.com.br

R. da Costa Lima
e-mail: r.c.lima@uol.com.br

T. Ogasawara
Department of Metallurgical and Materials Engineering, Federal University of Rio de Janeiro (COPPE/UFRJ), Rio de Janeiro, RJ, Brazil

This work focuses mainly on the use of TG, DSC and FTIR analyses for the characterization of the gel decomposition, resulting in the low temperature formation of $Ba_2Zn_2Fe_{12}O_{22}$ by the citrate sol–gel technique**.** A special thermal treatment after the self-combustion method and different calcination temperatures (850, 950 and 1000 °C) were used to evaluate their effect in the formation of $Ba_2Zn_2Fe_{12}O_{22}$ hexaferrite crystalline powders [3].

The use of the special thermal treatment before the calcination temperature was responsible for the total organic precursor elimination on the $Ba_2Zn_2Fe_{12}O_{22}$ single phase formation illustrated by X-ray diffraction (XRD) and confirmed by TG and X-ray fluorescence (XRF) analyses. The use of the thermal treatment also resulted in the formation of the desired magnetically soft nanoferrite as illustrated by FTIR, TG, XRD, XRF, VSM and FMR techniques.

In order to obtain the composites for the microwave absorption measurements the powders were mixed with epoxy resin resulting in the composition 80:20 (mass%, ferrite:epoxy). The microwave measurements were based on transmission/reflection method (T/R), using a rectangular waveguide.

Experimental

In the citrate precursor method the cations stoichiometric content in the aqueous solution reacts with the polyfunctional organic acid (citric acid) under controlled pH conditions to give an organometallic precursor complex. The citrate precursor decomposes at temperatures lower than 500 °C allowing barium hexaferrite to be formed at lower temperatures than the required by the powder mixing method besides providing an useful way for producing ultrafine homogeneous systems [5].

Ultrafine $Ba_2Zn_2Fe_{12}O_{22}$ hexaferrite powders were synthesized by this method using the analytical reagent grade $Fe(NO_3)_3{\cdot}9H_2O$, $Ba(NO_3)_2$, $Zn(NO_3)_2{\cdot}6H_2O$ and monohydrated citric acid in stoichiometric molar ratio. The preparation of the solutions was carried out weighting solids and placing then in a round bottom vessel. Bidistilled water was added to each one under agitation until total dissolution of solids.

The mixed solution containing the desired cations and citric acid was heated up to 80 °C. Ammonia solution was added drop wise into the solution to make it neutral or slightly alkaline (pH = 7.5) for subsequent precipitation of the expected organometallic complex that pops up after the water evaporation. Each of several key-metal cations reacted with citric acid under controlled pH conditions to give the respective metal citrate, making up an homogeneous joint metallic citrate precursor complex.

The mixed solution was rotoevaporated under vacuum at 100 °C to produce a highly viscous gel, and then ignited at approximately 250 °C temperature at which self-burning took place in accordance with the predetermined combustion temperature giving rise to loose powders [3]. The obtained powders were air calcined during 4 h at 850, 950 and 1000 °C after heating up at a rate of 10 °C min^{-1}. Then, the muffle-furnace was cooled down at 10 °C min^{-1} to the room temperature [5].

For the calcination temperature economically selected as ideal a special thermal treatment was introduced before the calcination step following the heating schedule: 2 °C min^{-1} up to 450 °C, a 450 °C plateau for 1 h, and then the muffle furnace was cooled down at 10 °C min^{-1} to the room temperature [1].

The $Ba_2Zn_2Fe_{12}O_{22}$ crystalline phase formation was investigated by X-ray diffraction (XRD), X-ray fluorescence (XRF), scanning electron microscopy (SEM), vibration sample magnetometry (VSM), thermogravimetric analysis (TG), differential scan calorimetry (DSC) and ferromagnetic resonance (FMR).

The calcined products were subjected to X-ray diffraction, with CuKα radiation, in order to assure the formation of the Y-type barium hexaferrite crystalline phase. A PANalytical X'Pert PRO X-ray diffractometer with a step speed of 1 min^{-1}, in the θ–2θ Bragg–Brentano geometry was employed.

X-ray fluorescence (XRF) measurements were carried out by using a Phillips model PW 2400 sequential spectrometer. This quantitative method was used to determine the stoichiometry of the ferrite samples, which were analyzed in the form of a fused bead using lithium tetraborate flux.

The infrared spectra were recorded using a FTIR spectrometer Nicolet Magna 760.

The thermal analyses were carried out in a Schimadzu-50 with heating rates of 10 °C min^{-1} in static air, while the morphological study was performed in a ZEISS Scanning Electron Microscope model DSM 940 A.

The 4500 VSM of E.G & G Princeton Applied Research was used to measure the magnetic hysteresis loops and FMR spectra were recorded at 9.52 GHz using a Varian Model E-9.

The microwave measurements conducted in this work were based on the Transmission/Reflection method (T/R) using a rectangular waveguide as the confining medium for the samples. Using the data obtained (ε', ε'', μ' and μ'' values) from each of the samples measured, an expected prediction of the microwave reflectivity levels for the sheet absorbers was made by illustrating the values of reflectivity (dB) versus frequency (GHz), using the HP 8510 network analyzer system. The materials were analyzed for the frequency range 8.2–12.4 GHz (X- band) [6].

Results and discussion

The DSC–TG curves of the the dried gel are illustrated in Fig. 1. The TG curve exhibits two mainly distinct mass loss steps. The first one in the temperature range of 40–180 °C, which is accompanied by a week endothermic peak around 160 °C in the DSC curve, corresponds to the loss of the residual water and volatiles. The second mass loss of ~70% between 180 and 220 °C exhibited as an abrupt fall in the TG plot is an evidence of the citrate decomposition during the self-combustion process, which is accompanied by the large exothermic double peak in the DSC curve corresponding to the metal oxidation. The combustion temperature was determined as 235 °C. At about 300 °C, the 6% mass loss is due to the oxidation reaction of the residual carbon. For temperatures above 440 °C, no further mass loss was observed, indicating the total elimination of organics.

Figure 2 illustrates the influence of the calcination temperature on the crystalline phase formation of $Ba_2Zn_2Fe_{12}O_{22}$.

The use of the lower temperature (850 °C) resulted in the presence of second phases, such as γ-Fe_2O_3 (JCPDS 00-089-5894) as illustrates Fig. 2. XRD analysis also indicated that at 950 °C $Ba_2Zn_2Fe_{12}O_{22}$ became clearly the predominant phase according to JCPDS 00-044-0207 and for this reason it was selected as the economically ideal calcination temperature, although second phases trace amounts undetectable by XRD analysis may be presented.

Figure 3 illustrates the effect of the thermal treatment in the organic precursor elimination evaluated by XRD.

The introduction of the special thermal treatment before the calcination at 950 °C was important for the total elimination of the organic precursor, assured by the disappearance of the baseline's roundness.

Results from X-ray fluorescence analysis (XRF) confirmed that the powders submitted to the special thermal treatment and calcined at 950 °C achieved the planned stoichiometry. The presence of carbon was not detected even in trace amounts indicating the total organic precursor elimination favoring the desired formation of $Ba_2Zn_2Fe_{12}O_{22}$.

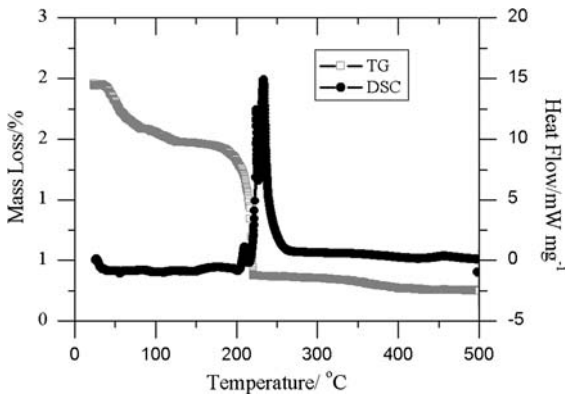

Fig. 1 TG and DSC curves of the dried gel

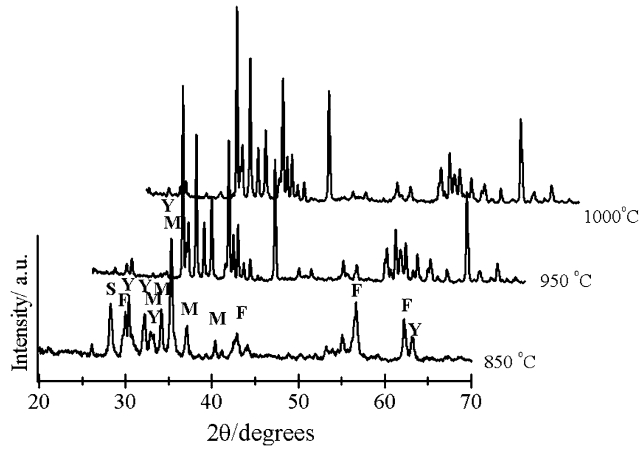

Fig. 2 X-ray diffraction curves for $Ba_2Zn_2Fe_{12}O_{22}$ powders calcined at different temperatures with Y and M hexaferrites plus S = $BaFe_2O_4$ and F = γ-Fe_2O_3

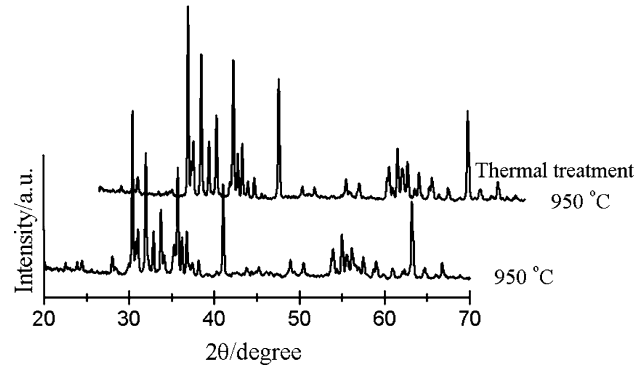

Fig. 3 X-ray diffraction curves for $Ba_2Zn_2Fe_{12}O_{22}$ powder calcined at 950 °C illustrating the effect of the thermal treatment

Chemical and structural changes and the desired crystal phase present in the material during combustion and calcination processes can be observed by FTIR characterization. Figure 4a shows the FTIR spectrum of the $Ba_2Zn_2Fe_{12}O_{22}$ dried gel indicating the characteristic bands of the O–H stretching vibration of water and citric acid in the 3,700–2,700 cm^{-1} range, while the anti-symmetrical and symmetrical stretching vibration bands of $-CO_2^-$ related to citric acid are located at about 1,620 cm^{-1}. The bands of NO_3^- located at 1,400–1,380 and 820 cm^{-1} are ascribed to the N=O stretching vibration and N–O bending vibration, respectively. After combustion and thermal treatment (Fig. 4b), the absorption band of O–H disappeared and $-CO_2^-$ and NO_3^- bands decreased drastically. Also in Fig. 4b) the absorption band at approximately 560 cm^{-1} is

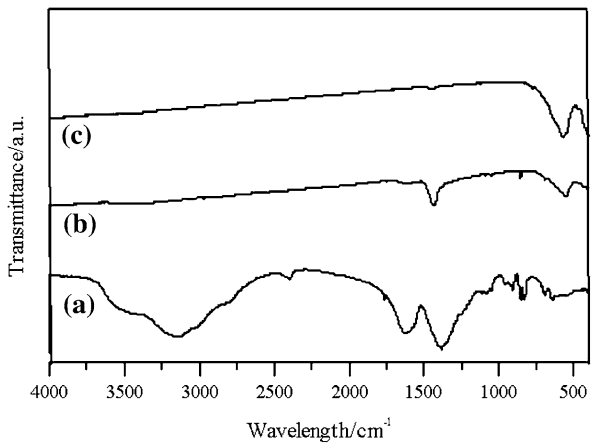

Fig. 4 FTIR spectra for (a) $Ba_2Zn_2Fe_{12}O_{22}$ dried gel, (b) powder after combustion and thermal treatment and (c) powder after calcination at 950 °C

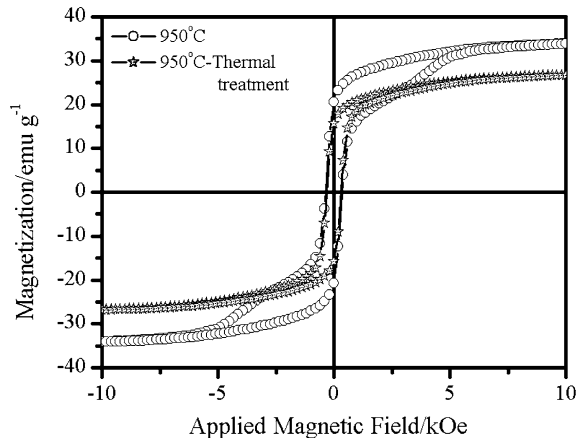

Fig. 6 Hysteresis curves for Y-type barium hexaferrite samples calcined at 950 °C

due to the iron–oxygen bonds, characterizing the presence of γ-Fe_2O_3, in accordance with XRD results (Fig. 2). The powder calcined at 950 °C (Fig. 4c) only revealed the well resolved absorption band at 580 cm^{-1} corresponding to the metal-oxygen stretching vibration of $Ba_2Zn_2Fe_{12}O_{22}$ single phase.

The hysteresis curves for Y-type barium hexaferrites calcined at 850, 950 and 1000 °C without the thermal treatment are illustrated in Fig. 5.

As it can be seen in Fig. 5, the hysteresis curves at 850, 950 and 1000 °C do not show typical features of magnetically soft ferrites due to the presence of second phases such as γ-Fe_2O_3 illustrated by XRD and FTIR analyses. The effect of the special thermal treatment before calcination at 950 °C on the hysteresis curves of $Ba_2Zn_2Fe_{12}O_{22}$ samples is illustrated in Fig. 6.

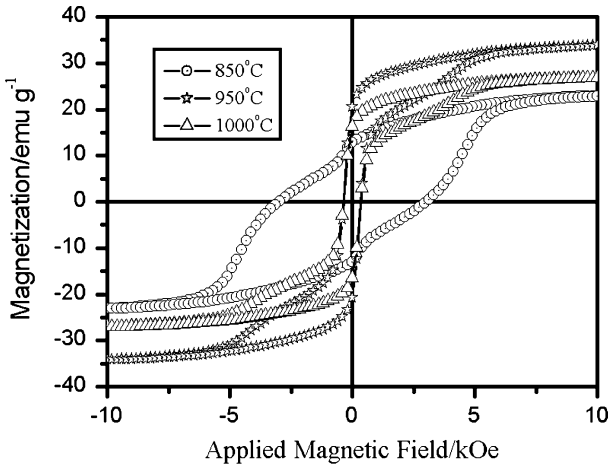

Fig. 5 Hysteresis curves for Y-type barium hexaferrites calcined at 850, 950 and 1000 °C without thermal treatment

The magnetization curve for the sample submitted to the special thermal treatment shows a completely different profile of the other curves with 26.59 emu g^{-1} of magnetization of saturation, being characteristic of a soft ferrite allowing its application as a microwave absorbing material (RAM).

Figure 7 illustrates the hexagonal-shaped morphology of $Ba_2Zn_2Fe_{12}O_{22}$ nanopowder thermal treated and calcined at 950 °C with an average particle size lower than 1 μm determined by the Scherrer equation.

The use of long calcination period of time (4 h at 950 °C) resulted in the beginning of the sintering process of some $Ba_2Zn_2Fe_{12}O_{22}$ nanoparticles.

Figure 8 illustrates the TG curves for the powders obtained after (a) combustion, (b) thermal treatment and (c) calcination at 950 °C.

After combustion the dried gel was transformed into a mixture of oxides, carbonates and the organic precursor. From Fig. 8a it can be seen at approximately 400 °C the total organic elimination and the barium carbonate

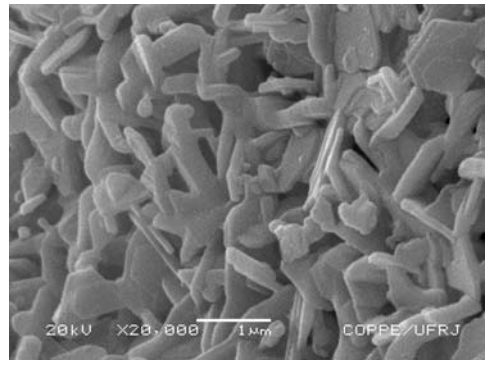

Fig. 7 SEM image of $Ba_2Zn_2Fe_{12}O_{22}$ ultra fine nanopowder

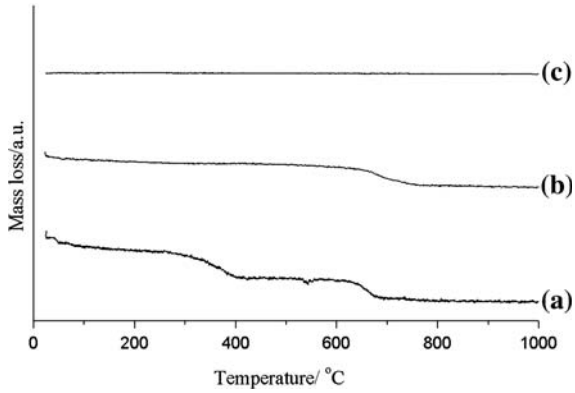

Fig. 8 TG curves for the powders obtained after (a) combustion, (b) thermal treatment and (c) calcination at 950 °C

decomposition at 650 °C. Figure 8b confirms the thermal treatment efficiency, illustrated by the complete disappearance of the organic mass loss. The $Ba_2Zn_2Fe_{12}O_{22}$ formation is confirmed by the thermal stability of the Y-type Zn-barium hexaferrite submitted to the special thermal treatment and calcined at 950 °C as illustrates Fig. 8c.

The effect of the thermal treatment on the FMR curves for the samples calcined at 950 °C is illustrated in Fig. 9.

In a nonoriented polycrystalline powder the crystals which are aligned with the applied magnetic field resonate at the same field value as a single crystal in the easy plane. All other crystallites require a greater field for resonance and so the absorption curve will be broadened in the direction of higher magnetic fields [2].

One of the consequences of the hexagonal structure is that high values of magnetic anisotropy can be attained with different Me substitutions. If the Me substitution and the thermal treatment make possible to find small values of FMR line width as 790 Oe obtained in this work, the material can be useful in the construction of microwave devices [2, 7, 8].

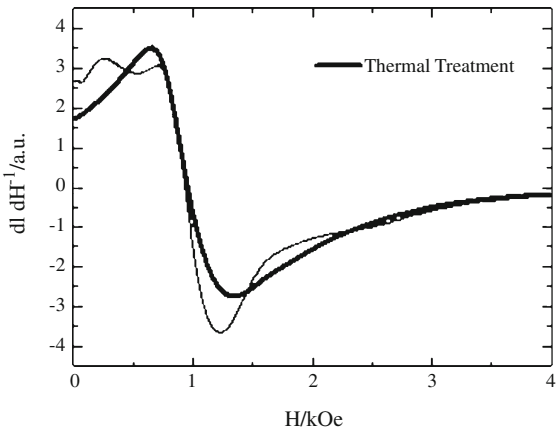

Fig. 9 Electron spin resonance of nonoriented $Ba_2Zn_2Fe_{12}O_{22}$ nanoparticles

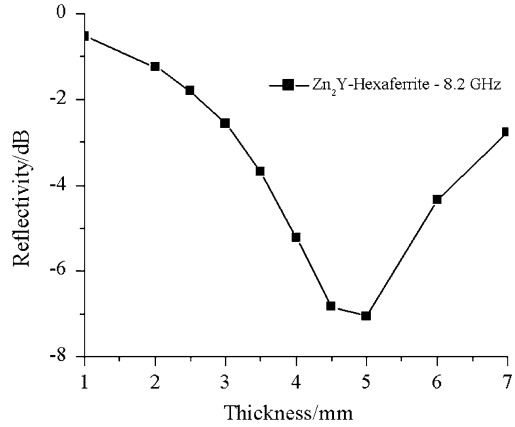

Fig. 10 Reflectivity results for the composite 80:20 of $Ba_2Zn_2Fe_{12}O_{22}$: epoxy resin, with different thickness

Moreover, as the particle size is sub-micron (Fig. 7) the microwave absorbing properties can be greatly improved. If the particle size of the absorber is in nanoscale and the discrete energy level spacing is in the energy range of microwave the electron can absorb the energy as it leaps from one level to another which may lead to the increment of attenuation [7–9].

According to the literature the addition of zinc ions brings about perfection in the hexaferrite crystal structure [10] and improves the magnetic properties of the ceramics making possible its use as a RAM for X/Ku bands [11].

Figure 10 illustrates the dependence of the reflectivity measurements on thickness. The best performance as a microwave absorbing material (RAM) for the X-band (8.2 GHz) was observed for the composite 80:20 of $Ba_2Zn_2Fe_{12}O_{22}$:epoxy resin, 5 mm thick.

Conclusions

In accordance with XRD, TG, FTIR and SEM results well defined $Ba_2Zn_2Fe_{12}O_{22}$ nanocrystalline powder was formed at 950 °C, using the self-combustion sol–gel method.

The use of the special thermal treatment before calcination at 950 °C assured the total elimination of the organic precursor as illustrated by XRD, XRF and TG results.

As the resonant line width of $Ba_2Zn_2Fe_{12}O_{22}$ was about 790 Oe, this soft magnetic ferrite is a promising candidate to be used as a microwave absorbing material (reflectivity of −7 dB and a microwave absorption of 80%) for the X-band (8.2 GHz), in composites with epoxy resin (80:20), 5 mm thick.

Acknowledgements The authors gratefully acknowledge the AMR-IAE for the reflectivity measurements and IF-UFRJ for the VSM analyses, as well as to CNPq, CAPES and FAPERJ for financial support.

References

1. Huang JG, Zhuang HR, Li WL. Synthesis and characterization of nano crystalline $BaFe_{12}O_{19}$ powders by low temperature combustion. Mater Res Bull. 2003;38:149–59.
2. Kwon HJ, Shin JY, Oh JH. The microwave absorbing and resonance phenomena of Y-type hexagonal ferrite microwave absorbers. J Appl Phys. 1994;75(10):6109–11.
3. Haijun Z, Xi Y, Liangying Z. The preparation and microwave properties of $Ba_2Zn_zCo_{2-z}Fe_{12}O_{22}$ hexaferrites. J Eur Ceram Soc. 2002;22(6):835–40.
4. Mentus S, Jelic D, Grudic V. Lanthanum nitrate decomposition by both temperature programmed heating and citrate gel combustion: comparative study. J Therm Anal Calorim. 2007; 90(2):393–7.
5. Mishra SK, Pathak LC, Rao V. Synthesis of submicron Ba-hexaferrite powder by a self-propagating chemical decomposition process. Mater Lett. 1997;32(2–3):137–41.
6. Obol M, Vittoria C. Measurement of permeability of oriented Y-type hexaferrites. J Magn Magn Mater. 2003;265(3):290–5.
7. Bady I. Ferrites with planar anisotropy at microwave frequencies. IEEE Trans Microw Theory Tech. 1961;MTT-9(1):52–62.
8. Nazarov AV, Cox RG, Patton CE. High power microwave properties of Zn-Y hexagonal ferrite—parallel pumping size effects. J Appl Phys. 2002;92:3890–5.
9. Ruan SP, Xu BK, Suo H, Wu FQ, Xiang SQ, Zhao MY. Microwave absorptive behavior of ZnCo-substituted W-type Ba hexaferrite nanocrystalline composite material. J Magn Magn Mater. 2000;212(1–2):175–7.
10. Haijun Z, Zhichao L, Chengliang M, Xi Y, Liangying Z, Mingzhong W. Complex permittivity, permeability, and microwave absorption of Zn- and Ti-substituted barium ferrite by citrate sol-gel process. Mater Sci Eng. 2002;B96:289–95.
11. Caffarena VR, Ogasawara T, Capitaneo JL, Pinho MS. Magnetic properties of Z-type $Ba_3Co_{1.3}Zn_{0.3}Cu_{0.4}Fe_{24}O_{41}$ nanoparticles. Mater Chem Phys. 2007;101(1):81–6.